EXPERIMENTAL PARTICLE ASTROPHYSICS

Michel SPIRO and Eric AUBOURG
DAPNIA/SPP, CEA/Saclay, 91191 Gif-sur-Yvette, France

Abstract

Experimental particle astrophysics is now a field of growing interest which is well established. These lectures discuss this field, apart from solar neutrinos. They address the issue of the dark matter problem. The high energy cosmic rays are also reviewed. The main experimental results obtained up to now are summarized. Prospects and new ideas are presented.

1. Introduction

In these lectures we discuss the field of experimental particle astrophysics, apart from solar neutrinos. The dark matter problem and high energy cosmic rays are reviewed. It The main experimental results obtained up to now are outlined. Prospects and new ideas are presented.

2. Introduction to dark matter

The estimate of the value of Ω, the ratio of the mean energy density in the Universe to the critical energy density, is one of the main issues in modern cosmology. We can measure the components of Ω in various ways :

- from luminous matter (stars), Ω_{lum},
- from the dynamical behavior of stars in spiral galaxies (galactic halos), Ω_{halo},
- from primordial nucleosynthesis (baryons), Ω_{bar}.

We know from observations that the contributions from dust or gas to Ω are negligible. The estimates for the values of Ω_{lum}, Ω_{halo} and Ω_{bar} are shown in figure 1 and compared to the magic value $\Omega = 1$ which is the preferred value for aesthetic and theoretical reasons (to avoid fine tuning in initial conditions, and to agree with inflation theories). From all these values, one can draw two main conclusions:

1) All these estimates are below 1. However, the value $\Omega = 1$ is not excluded, but in order to reach it, it seems unavoidable to invoke intergalactic non baryonic dark matter, such as WIMPs (Weakly Interacting Massive Particles: heavy neutrinos ν_H, or lightest supersymmetric particle LSP...), or light neutrinos such as 10 to 100 eV ν_e or ν_μ or ν_τ.

2) The comparison of the allowed range for Ω_{lum}, Ω_{halo} and Ω_{bar} suggests that

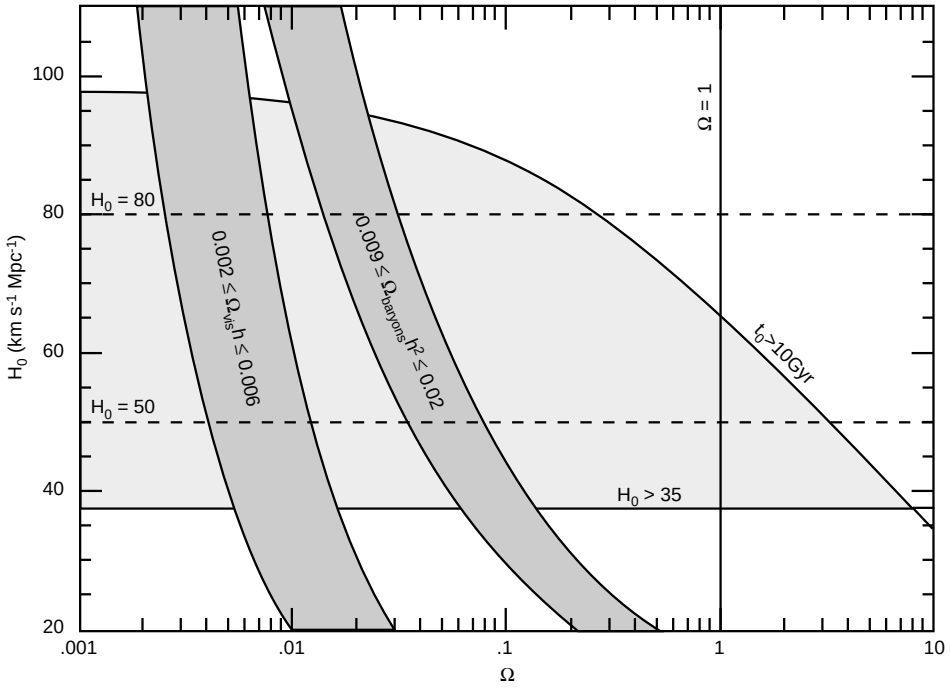

Figure 1: $H_0 - \Omega$ plot, indicating allowed (shaded in gray) and excluded regions. The fraction of visible matter in the Universe, Ω_{vis} is shown, along with the fraction of baryonic matter Ω_B resulting from nucleosynthesis, and the value $\Omega = 1$, theoretically preferred. The two current values for the Hubble constant: $H_0 = 50\,\mathrm{km\,s^{-1}\,Mpc^{-1}}$ and $H_0 = 80\,\mathrm{km\,s^{-1}\,Mpc^{-1}}$ are plotted in dotted lines. Two more limits are indicated: the lower bound $H_0 \geq 35\,\mathrm{km\,s^{-1}\,Mpc^{-1}}$ obtained from white dwarf stars and supernovae, and the lower bound on the age of the Universe $t_0 \geq 10\,\mathrm{Gyr}$ obtained essentially from the age of globular clusters.

baryonic dark matter is needed, and that the halos of spiral galaxies, like our own galaxy, could be partly or totally made of MACHOs (Massive Astrophysical Compact Halo Objects) which is almost the only possibility left for baryonic dark matter : these MACHOs could be either aborted stars (brown dwarves, planet like objects), or star remnants (white dwarves, neutron stars, black holes) [1].

3. Search for MACHO's with the gravitational microlensing technique

Very few possibilities remain for baryonic dark matter [2]. Cold fractal clouds of helium and molecular hydrogen have been suggested [3]. Primordial black holes are also a possibility. But probably the most plausible candidate would be compact objects too light to burn hydrogen, would-be stars beyond the main sequence. Their mass has to lie between the evaporation limit and the ignition threshold, *i. e.* $10^{-7}\,\mathrm{M_\odot} < M < 0.08\,\mathrm{M_\odot}$ [4, 5]. Those will be named MACHOs (Massive Compact Halo Objects) in the sequel.

A way to detect these MACHOs is to look for the temporary brightening of a star that occurs when a MACHO passes next to its line of sight.

3.1 The microlensing effect

The use of the microlensing effect to detect dark matter was first proposed in 1986 by Paczyński [6]. Figure 2 describes the phenomenon : a halo object D passes very close to the line of sight between the observer O and a distant star S – typically within a thousandth of an arc second.

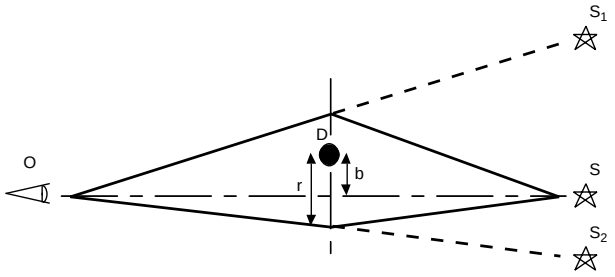

Figure 2: Instead of the direct ray going from the star S to the observer O, the deflector D causes the light to follow two distinct optical paths. The observer sees two images S_1 and S_2, usually non separable in the case of microlensing.

In the following, $L = OS$ and $x = OD/OS$. If the alignment was perfect, the observer would see an Einstein ring of radius R_E, with :

$$R_E^2 = \frac{4GML}{c^2}\, x(1-x) \tag{1}$$

More generally, the observer receives light through two optical paths, too close to be separated – the separation is also of about 10^{-4} arcsec. But since he received light that was emitted in a larger solid angle than without the deflector, the star appears brighter. It is easy to compute the apparent amplification from the deflection given by general relativity :

$$A = \frac{u^2+2}{u\sqrt{u^2+4}} \tag{2}$$

where u is the "reduced impact parameter", $d(OS,D)/R_E$.

Now, since the alignment needs to be so perfect, the effect is going to be sensitive to the movement of the deflector in the halo. If the deflector has a velocity v, which component transverse to the line of sight is $v_\perp$, and its trajectory has a minimum impact parameter u_o, then at any given time, we have:

$$u = \sqrt{u_o^2 + (\frac{v_\perp}{R_E}(t-t_o))^2} \tag{3}$$

and the phenomenon is time-dependent. It is convenient to define τ as $R_E/v_\perp$, the characteristic duration of the phenomenon. For stars in the Large Magellanic Cloud, the average duration is $<\tau>= 70$ days$\sqrt{M/\,\mathrm{M}_\odot}$. Figure 3 shows typical light curves.

For a given observed light curve, the measurable quantities are the maximum amplification, the duration, and the time of maximum. The amplification gives the impact parameter - which distribution must be flat -, but the duration is a function of the mass of the object, its speed, and its distance from the observer. For any given event, only

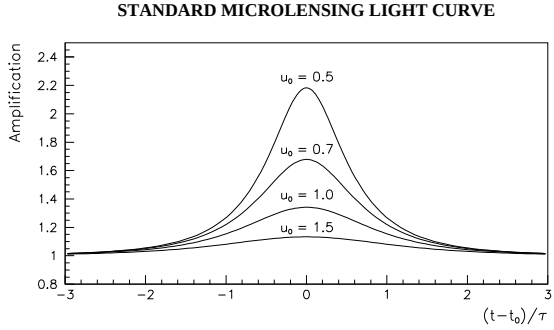

Figure 3: Some typical light curves. The abscissa is the time in unit of the time required for the deflector to move by an Einstein radius. The various light curves correspond to a reduced minimum impact parameter of 0.5, 0.7, 1.0 and 1.5 respectively.

a most probable mass can thus be computed. This mass is model-dependent, and the distribution around this most probable value is very broad. As statistics increases, it is however possible to perform a moment analysis to compute the moments of the MACHO mass distribution [5].

The probability of the microlensing phenomenon is computed by Paczyński [6] for stars in the Large Magellanic Cloud, and more generally in reference [7]. The idea is that the probability for a given star to be microlensed at a given instant by more than 34 % is simply the fraction of the sky covered by the Einstein radii of the MACHOs. Since the surface of the Einstein disk is proportional to the mass of the object, the total solid angle fraction - the optical depth - is independent of the mass of the objects. But since the event duration increases with the mass, lighter objects will cause more microlensing events in a given time period. Typically, for stars in the LMC and a "standard" halo, the optical depth is $\sim 0.5 \times 10^{-6}$. It is thus necessary to follow the luminosity of a few million stars.

Some basic properties of the microlensing effect will help to distinguish a signal from the background of variable stars:

• The light curve is symmetric and has a distinctive shape. Effects like binary deflectors can change the shape of an event, but the magnitude before and after the event must be the same.

• The effect is achromatic, since all photons follow the same geodesic. As most variable stars display color variations, this is a very powerful criterium, although effects like blending can render an event chromatic.

• The effect is rare enough to be unique for a given star. A long term follow-up of the candidates is therefore needed.

• The effect is independent of the physical properties of the microlensed star. In particular, the events must trace the spatial repartition of stars, as well as their repartition in the color-magnitude diagram.

3.2 The three experiments

3.2.1 EROS

EROS (Expérience de Recherche d'Objets Sombres) is a French collaboration of astrophysicists and particle physicists. The first phase consisted in fact of two experiments.

The first one was targeting high mass objects, and monitoring a few millions stars on a time scale of 30 mn, whereas the second experiment, aimed at low mass objects, was using CCDs to monitor fewer stars on a time scale of 30 mn.

The plate experiment was using the 1 m Schmidt telescope at the European Southern Observatory. Each 30 cm $\times$ 30 cm plate covers roughly an area of $5^\circ \times 5^\circ$ on the LMC. Two plates were taken each night, one with a blue filter, the other with a red filter. The exposure time was one hour.

The plates were then digitized by the MAMA at the Observatoire de Paris [8], and each yields 8×10^8 pixels of 0.7×0.7 arcsec^2. 56 plates have been taken in 1990-91, 200 in 91-92 and 25 in 92-93.

The CCD experiment was using a 16-CCD mosaic at the focal plane of a dedicated 40 cm telescope, in the dome of the GPO at La Silla. The CCDs were 576 $\times$ 405 pixel Thomson chips. The exposure times were 8 mn in R and 12 mn in B. During the 1991-92 campaign 2500 red and blue exposures have been recorded, and about 6000 during each the following campaigns (1992-93 and 1993-1994). About 10^5 stars have been monitored in the bar of the LMC.

In the second phase of the experiment, which just started in July 1996, the setup has been replaced by a dedicated 1m telescope, with a dual camera system and a dichroic beam splitter. Each camera is 4k$\times$8k pixels. Targets are the LMC and SMC, in order to increase statistics on long period events, and the Galactic bulge.

For all those programs, the photometric analysis is made with a specially developed algorithm, which needs to work well in crowded fields, be automated, and be fast enough to accommodate the huge volume of data. A reference image is first made by adding good images in each color. A catalog of stars is then produced, and the two colors are associated with a pattern matching algorithm. Then, for each image, the brightest stars are first identified and matched with the reference catalog, and are also used to determine the PSF. The geometric transformation is then used to impose the position of the stars on the measured image : this saves the star finding process, speeds up the PSF fit, which is then linear, and improves the photometric precision. Each photometric measurement is then added to the light curves of the stars for further analysis.

More details on the EROS experiment can be found in references [9, 10].

3.2.2 MACHO

The MACHO group is a University of California - CfPA Berkeley - Mount Stromlo Observatory collaboration. It uses a dedicated 50 inch telescope at MSSO, in Australia, with a dual camera system and a dichroic beam splitter, allowing simultaneous exposures in blue and red. Each camera has four 2048 $\times$ 2048 CCD, and covers a field of $0.7^\circ \times 0.7^\circ$. The camera system is described in detail in reference [11].

The observation strategy targets high-mass objects by surveying many fields: although the exposure time is about 5 mn, the sampling time scale is a day. 82 fields are monitored in the LMC. 21 in the SMC, and 75 in the bulge of the Galaxy. The experiment has started in 1992.

The photometric program, SoDoPhot, is based on DoPhot. As the EROS photometric algorithm does, it uses a template - the best image - to impose the position of stars.

Table 1: Characteristics of LMC events. For each event are given the unamplified magnitudes, the maximum amplification, and the duration in days.

Event	Magnitude		A_{max}	t (days)
MACHO 1	R=19.0	V=19.6	7.2	17.4
MACHO 4	R=19.8	V=20.0	3.00	23
MACHO 5	R=20.3	V=20.7	58	41
MACHO 6	R=19.3	V=19.6	2.14	44
MACHO 7	R=20.3	V=20.7	6.16	67
MACHO 8	R=19.8	V=20.1	2.24	31
MACHO 9	R=19.0	V=19.3	1.86	73
MACHO 10	R=19.2	V=19.4	2.36	21
EROS 1	R=18.7	B=19.3	2.5	26
EROS 2	R=19.2	B=19.3	3.3	30

3.2.3 OGLE

The OGLE experiment is a Warsaw-Carnegie collaboration, which observes the Galactic bulge in the Baade's window. It uses a non-dedicated 1 m telescope at Las Campanas Observatory, Chile, equipped with a 2048 x 2048 CCD camera. The data taking has started in 1992 and consists of images taken principally in I-band and only sparse measurements in V-band. The photometry uses a slightly modified DoPhot program [12].

3.3 Results

Once the light curves are built, all the collaborations are searching for a luminosity increase which is unique and achromatic, using roughly the same methods.

The CCD experiment of the EROS collaboration is the only program sensitive to low mass objects, in the range 10^{-7} to 10^{-3} $M_{\odot}$. No events have been found [10, 13], while about 30 are expected if the halo is made of objects of such a mass.

Both the EROS plate experiment and the MACHO experiment are looking for high mass MACHOs in the LMC. The EROS collaboration has reported 2 events [14, 9, 15], and the MACHO collaboration has reported 6 events [16, 17]. Table 1 summarizes the characteristics of these events.

The efficiency of the experiments has been determined, and the results are compared to the expectations. This is shown on figure 4 as an exclusion diagram for EROS and as a likelihood contour for MACHO [17]. One can see that the question of the amount of MACHO in our galactic halo can range from 20 to 100 per cent. It is above the expectations from known sources. The halo would contain stars just at the ignition threshold [18, 19] or even above like white dwarves [17].

As far as the Galactic bulge is concerned, the event rate is high enough that information quickly becomes obsolete ... At the time this article is written, the authors are aware of 12 events in the OGLE collaboration [20] and of more than 80 in the MACHO collaboration. The bulge rate is at least twice what would be expected for a "minimal disk" [7]. It could be compatible according to the MACHO collaboration with a "maximal disk" accounting for most of the velocity at the Sun radius [21]. On the other hand, the OGLE collaboration claims that its rate cannot be accounted for by any reasonable disk model, but that "a good case can be made for the lenses to be in the galactic bar, i.e.

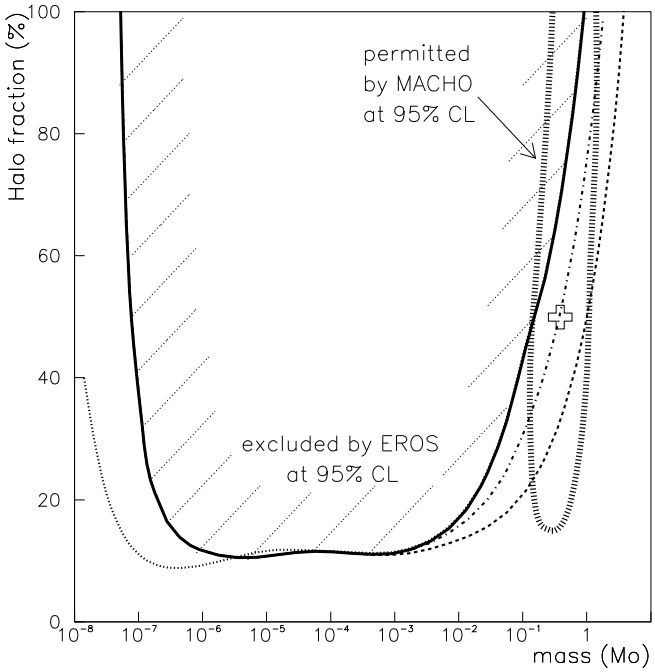

Figure 4: Exclusion diagram at 95 % CL for the reference model with all EROS data, assuming all deflectors to have the same mass. For the CCD program, we show the influence of blending and finite size effects (the dotted line on the left is the limit without those effects). Limits are shown for 0 (dashed line), 1 (mixed line) or 2 (full line) candidates assumed to be actual microlensing. The cross is centered on the area allowed at 95 % CL by the MACHO program assuming 6 microlensing events.

highly non-axially symmetric galactic bulge" [22]. More quantitative results should be available soon as the statistics increases.

3.4 Conclusion

Gravitational microlensing is a field in which a lot has happened in the previous year. All three collaborations have reported events which are compatible with microlensing.

Anyway, if the observed light curves are fully compatible with the theory of gravitational microlensing, and if the method has thus proved it was a worthy probe of low-mass star populations, some puzzling discrepancies in the event rates have occurred : compared to what is expected from having all the galactic dark matter in a spherical halo, the event rate towards the LMC is half too small, and the one towards the center of the Galaxy is twice too high.

The events rate towards the galactic bulge is high enough for more quantitative results to be available soon. For the LMC, a significant increase in the number of events is required to start doing any statistical analysis.

The MACHO collaboration is planning to continue to run for a few years with the same setup. The EROS collaboration has replaced its setup with a 1 m dedicated telescope, a dichroic beam splitter and two cameras, each fitted with 8 2048 $\times$ 2048 CCDs. The OGLE collaboration should soon have a dedicated 1.27 m telescope, with a

2048 × 2048 CCD, to be expanded later.

Three new other experiments have started now :

- DUO (photographic plates) directed towards the galactic bulge [23] ;
- AGAPE [24] and VATT which monitor pixels of M31.

4. WIMPs: lightest supersymmetric particle (LSP)

- Big Bang cosmology implies that if the contribution of cold dark matter particles to Ω , *i. e.* , $\Omega > 0.1$, these particles have interactions of the order of the weak scale, i.e. they are WIMPs, and supersymmetry through the lightest supersymmetric particle (χ) offers a natural candidate. Indeed one finds that the contribution of WIMPs to Ω depends only on their annihilation cross-section σ_A :

$$\Omega = \frac{3 \times 10^{-27}\,\mathrm{cm}^3\,\mathrm{sec}^{-1}}{\sigma_A v} \tag{4}$$

where v is the velocity at the time of decoupling and is roughly 1/4.

The annihilation cross section can be dimensionally written as α^2/m_χ^2, where α is the fine structure constant. It follows that for Ω around unity $m_\chi = 100\,\mathrm{GeV}$, the electroweak scale. There is a deep connection between critical cosmological density and the weak scale. The natural range of masses is expected to be

tens of GeV $< m_\chi <$ several TeV

- The natural scale of supersymmetry is below a few TeV, to provide a natural explanation of the hierarchy of the grand unification compared to the electroweak unification. Combined with LEP results, we find surprisingly the same allowed mass range as inferred from cosmological arguments, namely between 30 GeV and a few TeV.

4.1 Direct and indirect detection of WIMP's.

The hypothesis that dark matter particles are gravitationally trapped in the galaxy leads to the conclusion that, like stars, they should have a local Maxwell velocity distribution with a mean spread of 250 km/s. Then, the mean kinetic energy E_r received by a nucleus of mass M_n (in units of GeV) in an elastic collision with a dark matter particle of mass M_x is :

$$E_r = 2\,keV \times M_n M_x^2/(M_x + M_n)^2 \tag{5}$$

The energy distribution is roughly exponential. The expected event rate for elastic scattering on a given nucleus, assuming that 0.4 GeV/cm^3 is the local density of the halo (needed to account for the flat rotation curve of stars) depends only on the mass and interaction cross section.

Since the annihilation cross section is fixed in standard cosmology (around $10^{-36}\,\mathrm{cm}^2$, the elastic cross section on a nucleon is expected to be of the order of the annihilation cross section times the ratio of the phase space, namely the mass of the nucleon to the square (the reduced mass to the square) divided by the WIMP mass to the square. For a coherent interaction on a heavy nucleus target of mass A one expects an enhancement by A^4 if the neutralino is much heavier than the nucleus (coherence plus reduced mass effects).

These recoil events can be detected in well shielded deep underground devices such as semiconductor diodes, scintillators and cryogenic bolometers. Experimental limits on the cross section of WIMPs for scattering on germanium [25, 26], CaF_2 [27] and NaI [28] have been published. These limits are shown in figures 5 and 6, translated in terms of single nucleon effective cross section depending on whether we are dealing with pure axial coupling or with coherent N^2 coupling where N is the number of nucleons in the target nucleus.

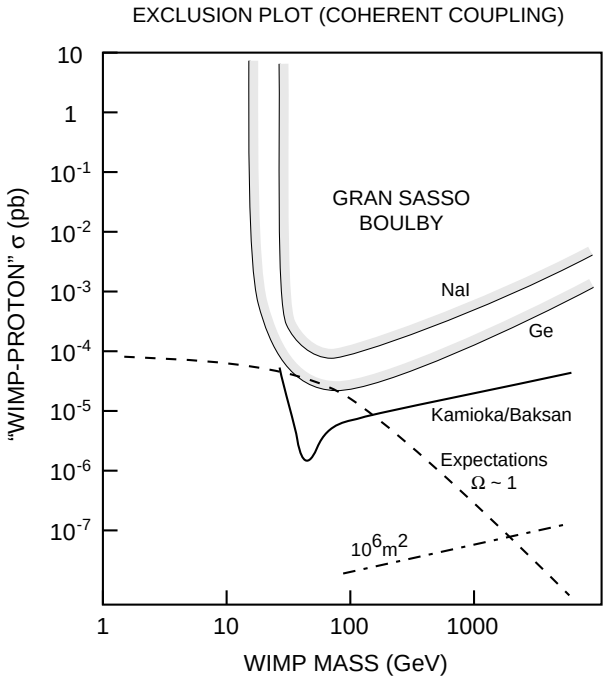

Figure 5: Effective elastic cross-section for coherent coupling. The expectations (dashed line) come from a naive estimate based on the annihilation cross section needed for $\Omega = 1$. They should be considered as giving the order of magnitude of the expectations.

To compare the sensitivity of the present experiments to the expectations, one can see that one approaches the required quality to detect with $S/N > 1$ the WIMP interactions if they interact coherently on the target (vector coupling) and have masses in the range of 100 GeV, but one has at least 3 to 4 orders of magnitude too high backgrounds to detect WIMPs with only axial coupling (spin dependent interactions).

Direct searches have no known fundamental limit on their background from radioactive impurities in the detector elements. Considerable progress has been made in lowering this background. Promising techniques to further eliminate the backgrounds include simultaneous detection of phonons and ionization in cryogenic germanium detectors [29], pulse shape analysis in NaI detectors and search for the expected seasonal variation (added velocity due to the movement of the Earth around the Sun) which will be ultimately necessary to confirm any observed signal [32].

WIMPs can also be seen indirectly by observing their annihilation products [30]. The most sensitive indirect technique uses the fact that WIMPs can be trapped in the Sun or the Earth. WIMPs with galactic orbits that happen to intersect an astronomical body will be trapped if, while traversing the body, they suffer an elastic collision with a nucleus

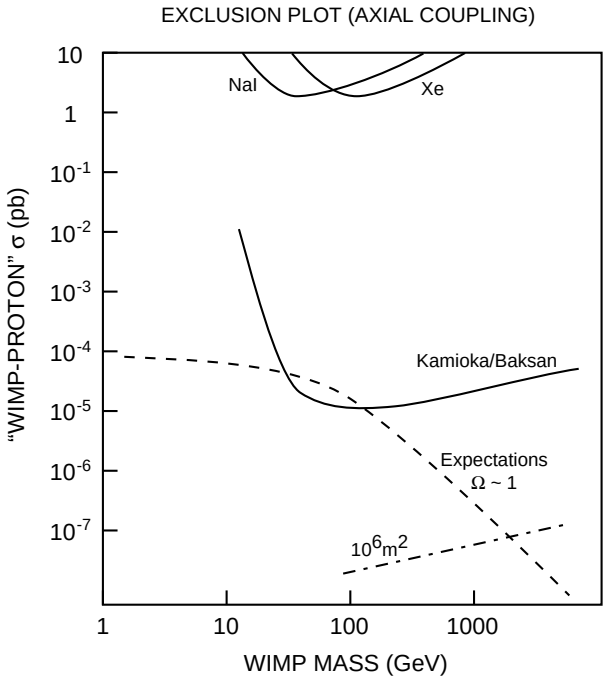

Figure 6: Effective elastic cross-section for axial coupling. The expectations (dashed line) come from a naive estimate based on the annihilation cross section needed for $\Omega = 1$. They should be considered as giving the order of magnitude of the expectations.

that leaves the WIMP with a velocity below the escape velocity [31]. The capture rate is proportional to the elastic cross sections on the nuclei of the astronomical body. A steady state will eventually be reached when the capture rate is balanced by the annihilation rate. Annihilations in the Sun or the Earth will yield a flux of high energy neutrinos either directly or by decay of annihilation products. The muon neutrinos can be observed in underground detector through their interactions in the rock below the detector yielding upward going muons pointing towards the Sun or the Earth. Presently, the most sensitive limits are those from Kamiokande [33] and Baksan [34]. The flux limits obtained so far on upward going muons can be interpreted in terms of a limit on the effective elastic cross section (figures 5 and 6). These can be then compared with the limits from direct searches.

Indirect detection experiments start to explore the highest part, in terms of cross section, of the neutralino domain, specially through coherent interactions (with Fe in Earth or Oxygen in the Sun). A new generation of neutrino telescopes of the size of $10^6\,\mathrm{m}^2$ would be perfectly adequate to reach the needed sensitivity for masses from 100 GeV to few TeV, for both coherent and spin dependent type of interactions. This relatively weak dependence on the WIMP mass is because the more massive are the WIMPs the more energetic are the neutrinos, the longer is the range of upwards going muons and the better is the angular resolution towards the sun). The threshold however might limit the sensitivity to low mass WIMPs.

For the future one can note that the indirect searches are limited by the fixed background from atmospheric neutrinos and can therefore expand their limits only in proportion of the square root of the exposure time or detector area. Their are now projects

of $1\,\mathrm{km}^3$ deep underwater or underice detectors which would be perfectly adequate for the indirect detection of WIMPs with masses greater than 100 GeV.

We conclude like J. Rich and C. Tao [35], Kamionkowski et al. [36] and Halzen [37] that the direct method might be superior if the WIMPs interact coherently and their masses are lower to 100 GeV. In all other cases, i.e. for relatively heavy WIMPs and for WIMPs with spin dependent interactions (or incoherent interactions), the indirect method is competitive or superior. The progress expected with indirect detection depends on the successful deployment of high energy neutrino telescopes of an effective area from 10^4 to $10^6\,\mathrm{m}^2$ with appropriate low threshold. The energy resolution of the neutrino telescope may be exploited to measure the WIMP mass and suppress the background. A kilometer-size telescope probes WIMP masses to the TeV range, beyond which they are excluded by cosmological considerations.

5. The case for light neutrinos

Although they are not favored by theories dealing with small scale structure formation (galaxy formation), 30 to 100 eV neutrinos are quite appealing to explain the nature of our halo [38].

Note that if our galactic halo is made of light neutrinos there should be a sharp resonant absorption line in the spectrum of ultrahigh energy intergalactic neutrinos reaching the Earth (figure 7). The detection of such a narrow line would be a proof of the neutrino halo. Its position would provide for the neutrino mass : $2\,M_\nu\,E_\nu\,=\,M_{Z_o}^2$. For a neutrino mass of 30 eV, the line would be around 10^{20} eV.

The ν_e is now excluded due to the severe upper limit on the mass (4.35 eV). However the ν_μ and ν_τ are perfectly viable candidates. Obviously the direct (laboratory or far supernova detection) or indirect (oscillations) measurements of the ν_μ and ν_τ masses are of crucial importance in the context of the dark matter problem. A likely scenario could be that the ν_τ is much heavier (30 eV) than the ν_μ and that the ν_μ is much heavier than the ν_e. In that sense the deficit of solar neutrinos could be a hint for neutrino ν_e-ν_μ oscillations and then for neutrino masses. The search for ν_μ-ν_τ oscillations in the range of Δm^2 of eV^2 to few hundred eV^2 (range of cosmological interest) has started at CERN with the CHORUS and NOMAD experiments. Even if the favored range of masses to explain the solar neutrino deficit is 10^{-4} to 10^{-2} eV, this could be the range of mass for the ν_μ, with a much lower mass for the ν_e and a much higher one for the ν_τ (30 eV). Neutrino masses could then both solve the dark matter and solar neutrino problems. Note also that the detection of the neutrino burst of a distant supernova through neutrino electron elastic scattering would be sensitive to the measurement of the ν_τ with the required sensitivity provided that there are more than a few thousand neutrino interactions detected.

6. The cosmic ray frontier

High energy cosmic rays - gamma-rays and charged particles - have always been a subject of common interest for astrophysicists and particle physicists. Indeed, the founding generation had their training in cosmic-rays physics. Various questions maintain this common interest :

- Where are the sites of acceleration ?
- What are the acceleration mechanisms ?
- What is the chemical composition (gamma, proton, or heavy nuclei) ?

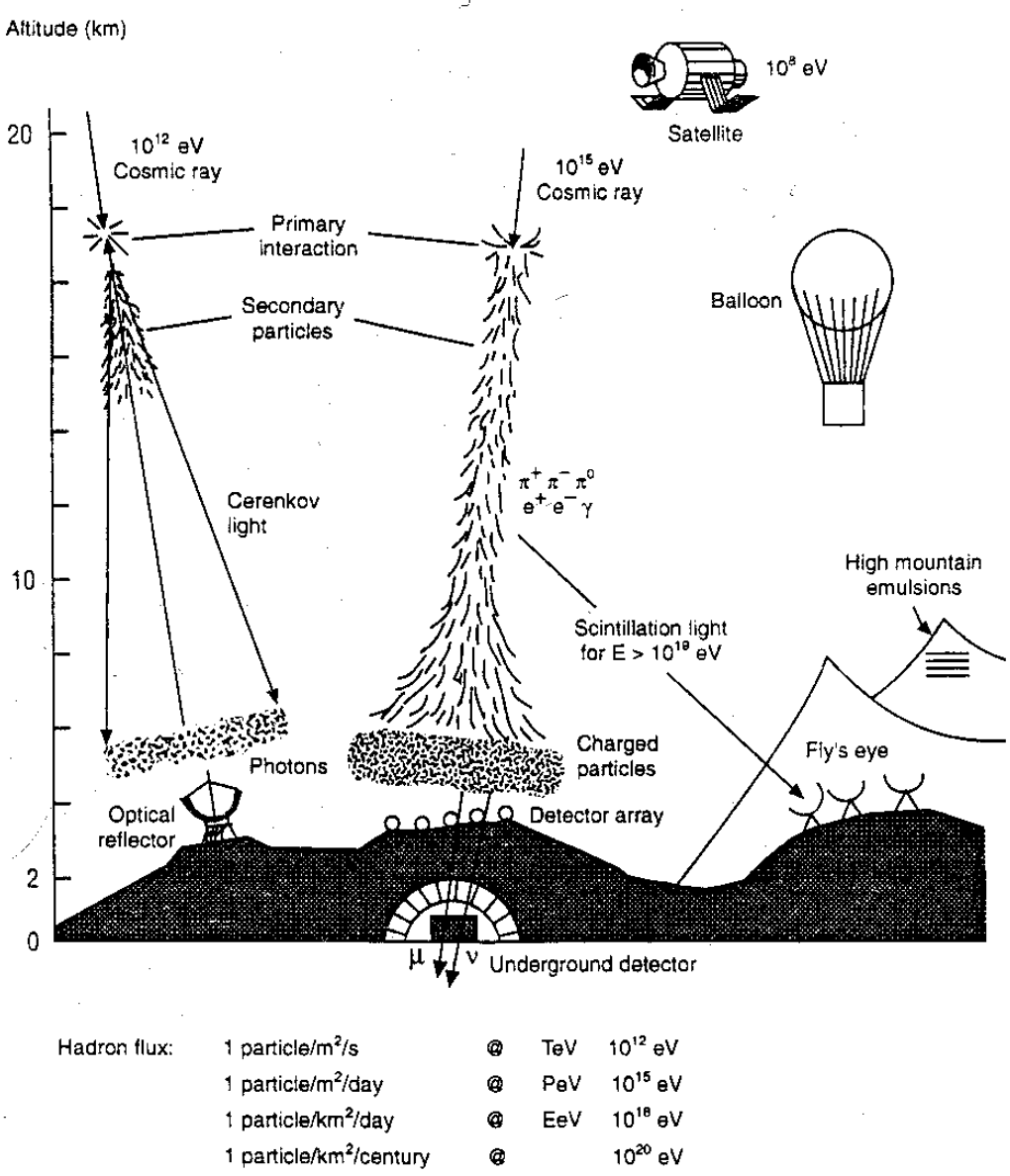

Figure 7: High energy cosmic rays detection techniques.

- What are the energy spectra, are there cut-off energies, and why ?

- Do we understand the interactions of the highest energy particles ?

- Are there particles in the cosmic rays which have not been found at the present accelerators ?

The study of cosmic rays - their energy spectrum, composition, and searches for point sources or preferred sites of acceleration - uses a wide variety of techniques (see figure 7) and attracts a large community (several hundred physicists) of relatively small groups throughout the world. The physics goals are promising and achievable.

Presently, a wide variety of experiments can be classified as taking place in the high, very high, ultra high and extreme energy regimes, each of which has an applicable detection technique. Experiments, below 20 GeV fall in the domain of satellite experiments. The range of experiments considered in this report are those above.

6.1 Gamma ray astronomy

a) Below 20 GeV (satellite experiments).

Below 20 GeV, the rate of particles impinging on the Earth's atmosphere is high enough to be detected by satellite experiments. For instance, the Compton Gamma Ray Observatory satellite, with its four instruments covering the 30 keV - 30 GeV energy range, has already provided many results, including some on gamma-ray bursts. A total of six pulsars (galactic sources) have been identified, and more than 40 active galactic nuclei (extra galactic sources) have been observed to be gamma-ray emitters. The statistics collected by the small sensitive area of satellites limit their energy domain at an upper value of 10-20 GeV.

b) From 20 GeV to 200 GeV gamma-ray astronomy (Cerenkov technique).

At this time, this is a region where no observations are possible up to the present 200-400 GeV threshold of ground-based atmospheric Cerenkov telescopes, which use the atmosphere as a giant calorimeter by observing the Cerenkov light radiated by the showers in the atmosphere. To fill the gap between 20 and 200 GeV, it has been proposed to collect the Cerenkov light from low energy gamma showers by many individual mirrors (e.g. the heliostats of solar power plants) focused onto a single light detector [40]. More sophisticated satellite experiments (like the GAMS or AMS project) can also and presumably better achieve this goal in a somewhat more distant future.

c) From 200 GeV to 10 TeV gamma-ray astronomy (Cerenkov technique).

Figure 8 summarizes the current state-of-knowledge of the gamma ray sky with two maps. On the left are shown sources with 0.1 ¡ E ¡ 20 GeV, detected by EGRET on CGRO. The figure on the right display sources with 0.3 ¡ E ¡ 15 TeV detected on the ground.

Above 200 GeV, reaching into the TeV region, is the domain of very high energy astronomy, which has been explored for many years by relatively simple detectors. One galactic source, the Crab Nebula, has been identified (by the Whipple [41] collaboration in the United States, by ASGAT, and by the Thémistocle collaboration in the French Pyrénées). A pulsar also has been observed in the Southern Hemisphere (PSR 1706-44) by a Japanese group. Detailed studies of the energy spectra of such sources should shed light on the acceleration mechanisms of cosmic rays in neutron stars.

Whipple's observation, few years ago, of the extragalactic source Mrk 421 in the

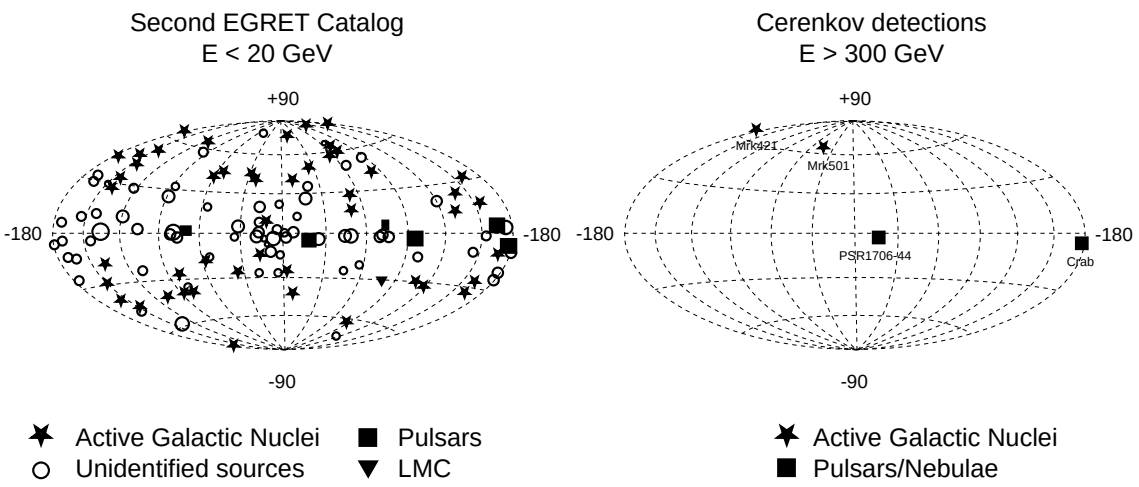

Figure 8: Sky maps of gamma ray point sources, in Galactic coordinates (from reference [40]).

TeV region [42] has opened the possibility of studying the acceleration mechanisms in active galactic nuclei and of probing the absorption due to gamma-gamma interactions with the diffuse infrared background radiation.

The spectrum of gamma rays from the Crab nebula, from 100 keV to 100 TeV is shown in figure 9, along with a one-parameter fit to a model covering most of that range. The data comes from the GRIS balloon experiment, from the COMPTEL and EGRET instrument aboard CGRO, from six different Cerenkov experiments operating over a range of energies, while upper limits from scintillator array experiments are also shown. Generally, non-pulsed gamma ray fluxes are assumed to come from the nebula, as opposed to the pulsar. The model used by deJager and Harding [39] is based on the acceleration of electrons in the shock wave formed where the particle wind from the pulsar is stalled by the nebula. The inverse Compton scattering of the soft synchrotron photons radiated in the nebular magnetic field by the same parent electrons produces a characteristic spectrum in the GeV-TeV range. The cut-off energy of the Crab pulsar spectrum may have been measured by HEGRA recently around 10 TeV. It has been reported at this conference.

Whipple's observation, few years ago, of the extragalactic source Mrk 421 in the TeV region has opened the possibility of studying the acceleration mechanisms in active galactic nuclei (AGN) and of probing the absorption due to gamma-gamma interactions with the diffuse infrared background radiation.

A single model (see the CELESTE proposal [40]) unifying the great diversity of AGNs has been developing over the last decade or more. In its simplest form, those few percent of galaxies with an active nucleus would consist of a supermassive black hole (10^6 to 10^9 solar masses) surrounded by a disk of gas. The gravitational potential energy of the disk is converted to radiation energy as the matter accretes. The different types of AGNs - quasars, Seyferts, and so on - arise from variations of two quantities. One is the angle of the disk relative to an earthbound observer. The disk masks energetic phenomena occurring near the black hole (figure 10), so that AGNs viewed on-edge have thermal spectra peaking at longer wavelengths, while AGNs viewed along the disk axis give the

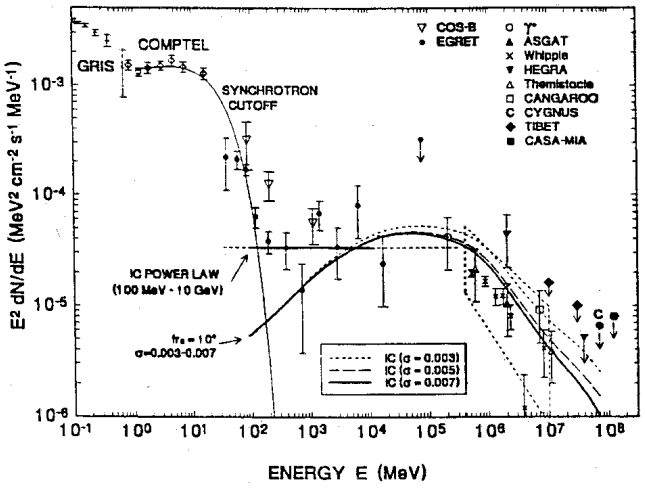

Figure 9: Energy spectrum of gammas from the Crab Nebula (from [39]).

observer a view to the heart of the engine. Secondly, a fraction of AGNs are observed to have a relativistic jet (presumably) aligned along the disk axis, in which plasma emitted from the core of the AGN travels nearly rectilinearly at bulk Lorentz factors of up to 10, terminating in radio lobes at distances of up to hundreds of kiloparsecs from the AGN core. Due to the large Lorentz factors of the photo-emitting plasma within the jets, those AGNs whose jets are pointing within several degrees of our line-of-sight will have have their apparent luminosities and observed time variabilities kinematically enhanced by orders of magnitude. This is believed to be geometry responsible for the blazar subclass of AGN, which exhibit rapid flux variability in essentially all measured frequency bands, from radio to gamma rays.

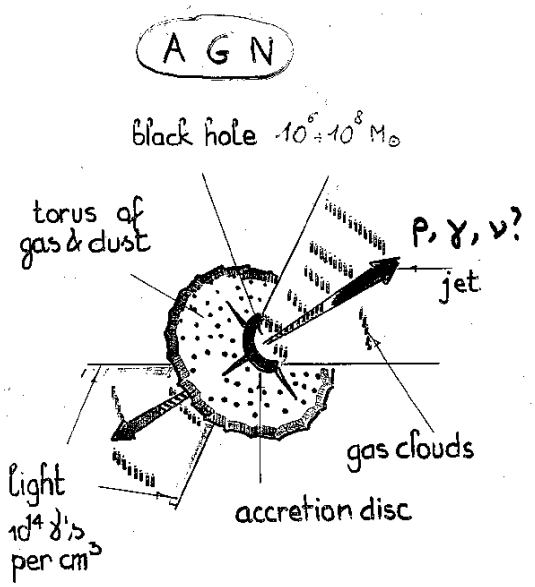

Figure 10: Schematics of an Active Galactic Nucleus (AGN) (from F. Halzen [46]).

A paradox seems to show up in figure 8. Yet, the EGRET AGN which has been

detected from the ground, Mrk 421 is amongst the dimmest for EGRET. The other AGN detected from the ground is even fainter and EGRET has been unable to see it. The fact that Mrk 421 is the closest EGRET AGN, and that Mrk 501 is as close (redshift z near 0.03 for both), is needed to explain the apparent contradiction : gamma ray absorption via e^+e^- pair production on the extragalactic infrared photon background. Here, we clarify this important point with figure 11, which shows the optical depth and so the cut-off in energy as a function of the redshift. Mrk 421 and 501 are not the brightness ones seen by EGRET but the closest ones. Finally, figure 12 illustrates the good flux sensitivity of Cerenkov detectors. It is the light curve of a gamma ray flare of Mrk 421, and the eight-fold increase in intensity over a few hours confirms the highly variable nature of blazars. This variability is presumably due to supermassive coalescence which could be the source low frequency gravitational waves and could be detected by the space interferometer LISA planned for 2015. This is reminiscent of the low energy gamma ray bursts (MeV range, ¡ 1 s duration) which might be associated with neutron stars coalescence with emission of high frequency gravitational waves which could be detected with ground based antennas like VIRGO and LIGO.

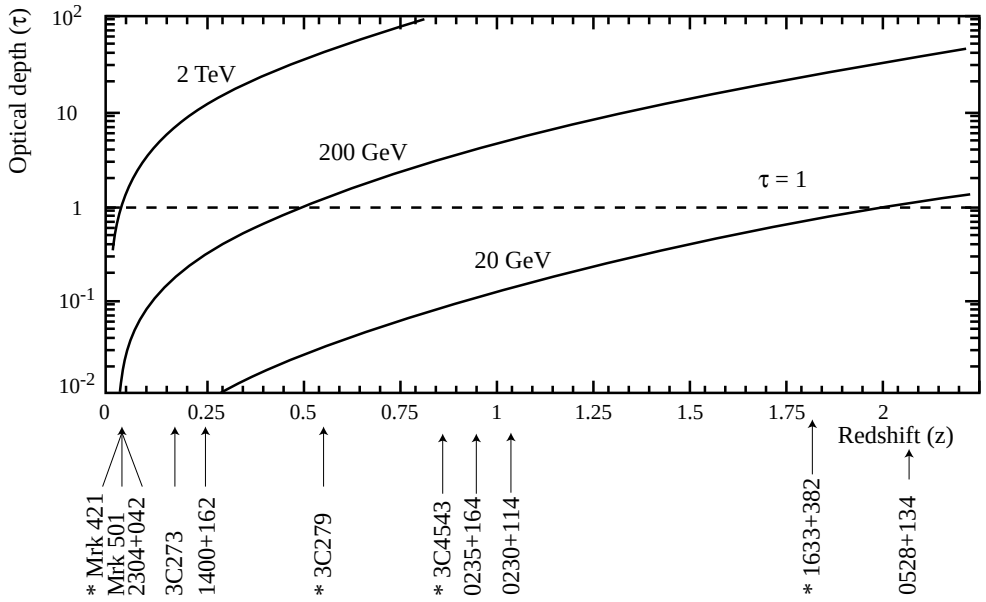

Figure 11: Number of interaction lengths for pair production as a function of the redshift

An important goal, which could also be reached in this energy range, is the discovery of the annihilation products of dark matter coming either from the halo or from the center of our Galaxy. In one scenario, the lightest supersymmetric (SUSY) particle dominates the dark matter of the galactic halo. Future detectors may be sensitive to the annihilation of SUSY particles into two gammas near the galactic center. The signature would be a monoenergetic gamma-ray line around the mass of the lightest supersymmetric particle. An enhancement of radiation could be observed towards the center of our Galaxy. Calculations show that a detector of 45 000 m^2 is required to get a significant signal-to-noise ratio.

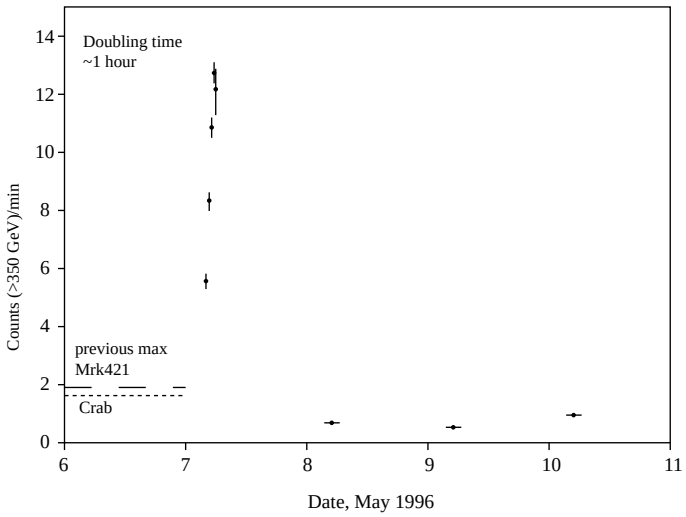

Figure 12: Mrk 421 burst as seen by Whipple [45].

6.2 Ultra and extreme high energy cosmic rays

a) From 50 TeV to 100 PeV astronomy (scintillation arrays).

At higher energies (ultra high energy, from around 100 TeV, 1 PeV, 1 PeV = 10^{15} eV), where charged particle showers can penetrate the atmosphere and reach the ground, it is possible to measure directly the direction (by timing) and the energy (by pulse height) of air showers with arrays of particle detectors, usually scintillators. Due to the higher energy threshold of the detectors, these devices have to deal with smaller fluxes but compensate by enlarging the surface of the array. Very large arrays have been recently put into operation. A vast quantity of statistics has been accumulated by HEGRA in the Canary Islands and by Cygnus I and Casa Mia in the United States. These three large arrays have now been joined by a fourth in Tibet which compensates for its smaller size by its very high altitude. These telescopes are all dense arrays of charged particles detectors.

The energy spectrum of the primary cosmic rays shows a knee around 10 PeV (figure 13). These cosmic rays are primarily charged particles (protons or nuclei). They have been bent by our galactic magnetic field and we cannot infer from their arrival direction, the direction of their site of acceleration. The dN/dE is proportional to $E^{-2.7}$ below 10^{16} eV but proportional to E^{-3} for E above it. The reason for the knee is unknown. It might be associated with a change of the cosmic ray composition from primarily hydrogen (H) to an enrichment in heavy nuclei (Fe). For a given energy primary, H has a higher magnetic rigidity and can therefore leak out of the galactic magnetic field more easily than a heavy primary.

It is generally believed that below the knee, cosmic rays have a galactic origin, presumably supernovae remnants.

b) Above 10 PeV.

Beyond 10^{16} eV (the extreme energy range), two detection techniques are used : air scintillation (the Fly's Eye technique) and giant arrays of sparse detectors, as at Akeno in Japan, Yakutsk in Russia, Sydney in Australia, and Hqverah Park in the United Kingdom.

No clear gamma-rays signal has bee observed by the Fly's Eye collaboration in the

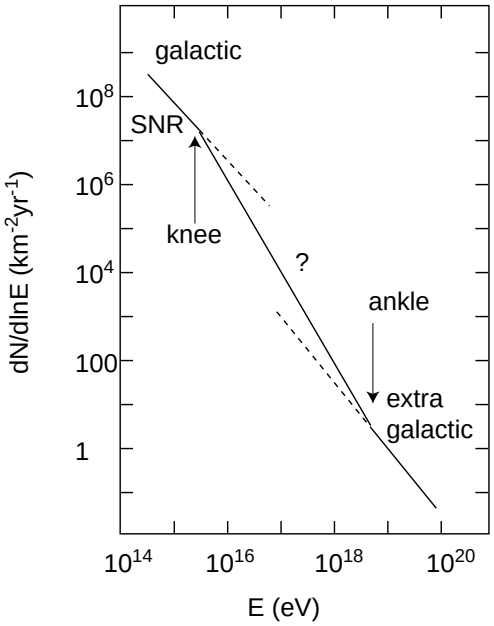

Figure 13: Energy spectrum of the primary cosmic rays.

United States.

Important results on charged hadrons (primary cosmic rays) have been reported. A flattening of the energy spectrum around 10^{18}-10^{19} eV (the Ankle) has been observed by Fly's Eye.

It is probably associated with a change from a predominantly heavy to a predominantly light composition.

The remaining questions are : is there a galactic disk excess, are there point sources, and what is the exact energy cut-off ? A cut-off is expected because of the interactions of extreme energy protons or heavy nuclei with the photons of the primordial microwave background (pion photoproduction). Beyond 50 Mpc all protons have energies ¡ few 10^{20} eV whatever their initial energy [44] (figure 14). This seems to be corroborated by the few observations above 10^{20} eV which show a non uniform distribution indicating a possible local supergalactic plane origin and non cosmological distances origin. At the extreme energies, neutrons can reach the Earth from everywhere in the local group without decaying : a neutron with10^{20} eV energy has a mean decay length of 1 Mpc. This opens up the possibility of a new astronomy. To get sufficient statistics to sort out the different scenarios, detectors with an area of 10 000 km2 are needed, like the Auger project [47].

6.3 Neutrino astronomy.

The open question of whether electromagnetic or hadronic processes dominate gamma-ray production mechanisms links gamma ray astronomy to the generation of neutrino telescopes now under design (Lake Baikal, Amanda, Nestor, Antares).

It is very possible that high energy cosmic ray above the ankle (10^{17} eV) are powered by AGN. The idea is very compelling because AGN are also the sources of the extragalactic highest energy photons detected with air Cherenkov telescopes. A relatively model-independent estimate of the required telescope area can be made by computing the expected neutrino rate from the assumption that the observed EeV cosmic rays are

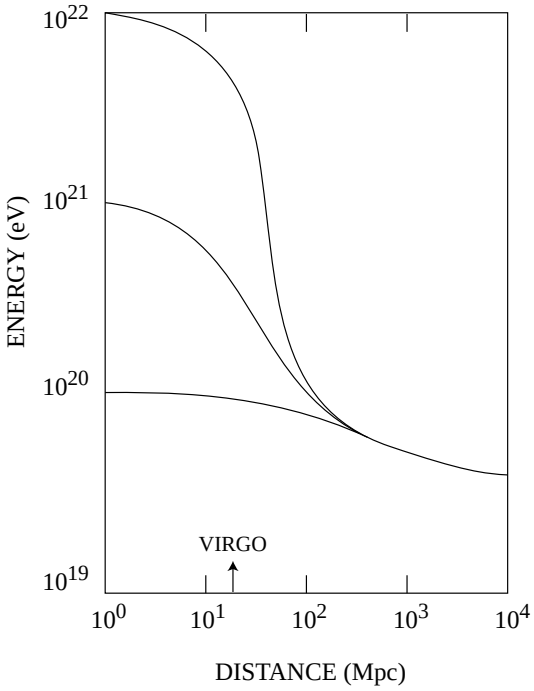

Figure 14: Degradation of the primary energy of a cosmic ray as a function of the distance, due to the interaction with the 2.7 K radiation.

produced by AGN [46]. It is very natural to assume in the scenario where this neutrinos are produced by high energy protons in the AGN jets interacting with the UV photon target, that roughly one neutrino is produced per every accelerated proton in the beam (figure 15).

The expected flux on Earth assuming an E^{-2} neutrino spectrum, assuming that the cosmic rays above 10^{17} eV (above the ankle) are coming from AGN, and assuming an equal luminosity in neutrinos and in charged cosmic rays above that energy, one expects a flux of neutrinos from AGN above 1 TeV of:

$$EdN/dE = \frac{10^{-9}}{E(TeV)}\, cm^{-2} s^{-1} sr^{-1} \tag{6}$$

The probability to detect a TeV neutrino is roughly:

$$P = R/\lambda = 10^{-6} E^2\, (TeV^2) \tag{7}$$

where R is the range of the muon and λ is the interaction length. Combining the two equations we obtain that neutrino detectors with $10^6\,m^2$ are required for observing 100 upwards going muons per year and detect sources with few muons (10 from a nearby source). The background of atmospheric neutrinos should be small (see figure 16). This type of detector is very similar to the one required for the indirect detection of cold dark matter WIMPs.

In summary, there is a natural possibility that AGN are the sources of the highest energy cosmic rays and could be detected both with high energy gamma detectors and neutrino detectors. Deep insights could then come simultaneously from giant air shower

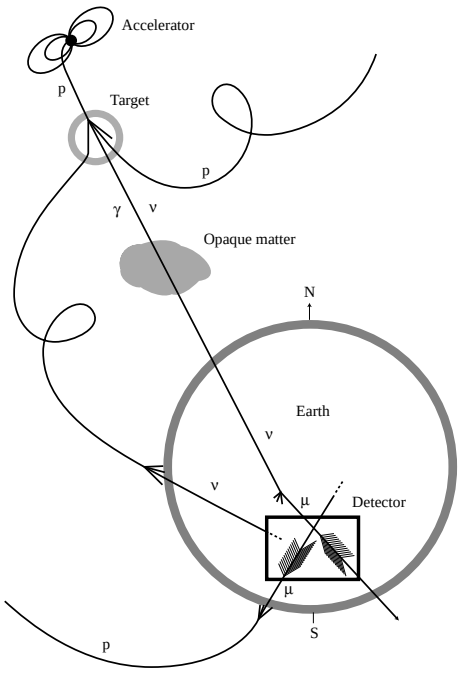

Figure 15: Neutrino production by AGN

array (like Auger), from deep underwater or underice neutrino detectors and from gamma-ray astronomy.

6.4 Antimatter

Search for antimatter in space, which could sign the existence of antistars through the detection of $\bar{\text{He}}$ and $\bar{\text{C}}$ is being undertaken vigorously. This is the AMS space shuttle and then space station experiment [43]. It will use a magnetic spectrometer with particle identification.

7. Conclusion

The field of experimental particle astrophysics is growing rapidly. The main challenges are solar neutrinos, dark matter, high energy cosmic rays, antimatter in space, gravitational waves. This builds a bridge between particle physicists and astrophysicists and complements particle physics with accelerators. We have to be opened to the idea that fundamental physics can be learnt from space and also in space.

It is a pleasure to thank the CELESTE collaboration, J. Ellis, F. Halzen, M. Jacob, R. Plaga, J. Rich and D. Vignaud for fruitful discussions, comments and the use of some of their documents. We thank N. Palanque for the figures.

REFERENCES

[1] B.J. Carr, Ann. Rev. Astron. Astrophys. 32 (1994) 531.
[2] R.F. Carswell et al., Mon. Not. R. Astron. Soc. 268 (1994) L1.
[3] D. Pfenniger and F. Combes, Astronomy and Astrophysics 285 (1994) 94.

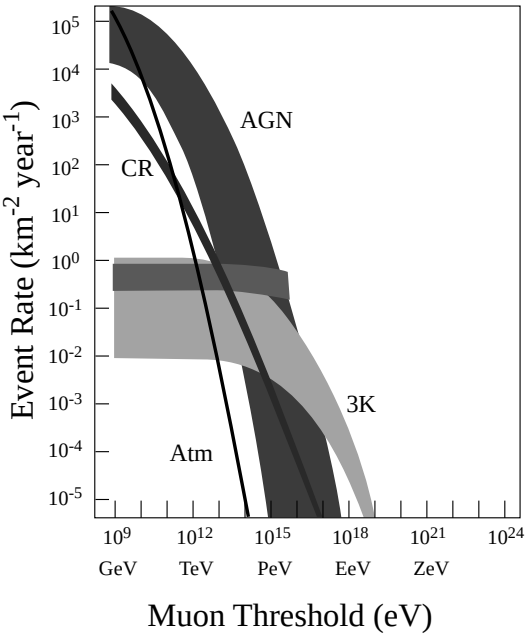

Figure 16: Expected muon energy spectrum (flux) due to neutrino interactions below deep detectors

[4] A. De Rújula et al., CERN report TH.5787/91, 1991.
[5] A. De Rújula et al., Astronomy and Astrophysics 254 (1992) 99.
[6] B. Paczyński, Astrophysical Journal 304 (1986) 1.
[7] K. Griest, Astrophysical Journal 366 (1991) 412.
[8] J. Berger et al., Astron. Astrophys. Suppl. Ser. 87 (1991).
[9] Cavalier F., *Recherche de naines brunes dans le halo galactique par effet de lentille gravitationnelle. Analyse des données photographiques de l'expérience EROS.* PhD thesis, Université Paris 11 Orsay, 1994.
[10] C. Renault, *Recherche de matière noire galactique par effet de microlentille gravitationnelle sous forme d'objets compacts de faible masse.* PhD thesis, Université Paris 11, 1996.
[11] C. Stubbs et al., SPIE Proc., 1900:192, 1993.
[12] P.L. Schechter et al., Pub. Astr. Soc. Pacif., 105 (1993) 1342.
[13] C. Renault et al., EROS Collaboration, in preparation, 1996.
[14] E. Aubourg et al., Nature 365 (1993) 623.
[15] R. Ansari et al., Astronomy and Astrophysics, to appear, 1996.
[16] C. Alcock et al., Nature 365 (1993) 621.
[17] C. Alcock et al., preprint, submitted to Ap. J., 1996.
[18] C. Alcock et al., Phys. Rev. Lett. 74 (1995) 2867.
[19] R. Ansari et al., Astronomy and Astrophysics 299 (1995) L21.
[20] B. Paczyński, preprint astro-ph 9411004, 1994.
[21] C. Alcock et al., Ap. J. Lett., 1994.
[22] B. Paczyński et al., Ap. J. Lett. 435 (1994) L113.
[23] C. Alard et al., Astronomy and Astrophysics 300 (1995) L17.
[24] P. Baillon et al., Astronomy and Astrophysics 277 (1993) 1.
[25] S.P. Ahlen et al., Physics Letters B195 (1987) 603.

[26] D. Reusser et al., Phys. Lett. B255 (1991) 143.
[27] C. Bacci et al., Phys. Lett. B293 (1992) 460.
[28] G. Davies et al., Phys. Lett. B322 (1994) 159 ; P. F. Smith et al., Phys. Lett. B379 (1996) 299.
[29] A. Lu et al., XXXI Rencontres de Moriond, January 20-27, 1996, Ed. Frontieres
[30] J. Silk et al., Phys. Rev. Lett. 55 (1985) 257.
[31] W.H. Press and D.N. Spergel, Ap. J. 296 (1985) 679.
[32] C. Bacci et al., Astroparticle Physics 2 (1994) 117.
[33] M. Mori et al., Phys. Rev. D48 (1993) 5505.
[34] M.M. Boliev et al., Nucl. Phys. B (Proc. Suppl.) 48 (1996) 83.
[35] J. Rich and C. Tao, report DAPNIA/SPP 95-01, Saclay
[36] M. Kamionkowski et al., Phys. Rev. Lett. 74 (1995) 5174.
[37] F. Halzen , Direct and Indirect Detection of WIMPs, preprint MAD/PH 95-887, June 1995
[38] R. Cowsik and J. Mac Clelland, Phys. Rev. Lett. 29 (1972) 669.
[39] A. K. Harding and O. C. De Jager, Ap. J. 396 (1992) 161).
[40] CELESTE Experimental Proposal, March 1996
[41] T.C. Weekes et al., Ap. J. 342 (1989) 379 ; G. Vacanti et al., Ap. J. 377 (1991) 401.
[42] M. Punch et al., Nature 358 (1992) 477.
[43] Antimatter Magnetic Spectrometer proposal, S. Ting et al., 1995.
[44] J. Cronin, Particle Astrophysics, Blois 1992, Editions Frontières.
[45] J. A. Gaidos et al., Nature 383 (1996) 319.
[46] F. Halzen, AGN as Particle Accelerators, preprint, MAD/PH/96, August 1996
[47] Auger proposal, 1996